

05.1;15.2

## Bending test of nanoscale consoles in atomic force microscope

© A.V. Ankudinov<sup>1</sup>, M.M. Khalisov<sup>1,2</sup>

<sup>1</sup> Ioffe Institute, St. Petersburg, Russia

<sup>2</sup> Pavlov Institute of Physiology, Russian Academy of Sciences, St. Petersburg, Russia

E-mail: alexander.ankudinov@mail.ioffe.ru

Received September 1, 2021

Revised October 18, 2021

Accepted October 20, 2021

Consoles and bridges of  $\text{MgNi}_2\text{Si}_2\text{O}_5(\text{OH})_4$  nanoscrolls were tested for bending in atomic force microscope. Using test data, we analyze how the consoles or bridges were fixed, and took this information into account when calculating the Young's modulus of the nanoscrolls. The results on the consoles are in good agreement with the results on the bridges when modeling the latter as three-span beams, and the former as beams on an elastic foundation with a suspended console.

**Keywords:** AFM, nanoscroll, bending, Young's modulus, Krylov's functions.

DOI: 10.21883/TPL.2022.02.52839.19010

The Young's modulus of a suspended quasi-one-dimensional nanoobject (tube, rod, scroll) may be determined with an atomic force microscope (AFM) by performing a bending test [1]. Consoles and bridges form as a result of drying out of a colloidal droplet of tested objects on various substrates with depressions [2,3]. The technique is based on AFM measurements of the stiffness profile of the object and the theory of small deflection of rods [4]. Unknown fixing conditions are the primary source of measurement error. The calculated values of the Young's modulus of a bridge regarded as a supported beam and a fixed-end beam differ by a factor of 4. This uncertainty is resolved [5,6] by comparing the measured stiffness profile to the profile of the center span of a model three-span beam (Fig. 1, *a*, top). If we extend the side spans, the center span goes smoothly from the fixed-end state to the supported state. The value of  $\lambda = L/l$  matching the theory to the measurement data is used to correct the Young's modulus. In actual practice, both the suspended object and the substrate may be deformed. A model with an elastic foundation supporting the object (Fig. 1, *a*, bottom) then becomes applicable. However, this model lacks a compact formula for the stiffness profile [7]. Both bridges and consoles were subjected to AFM bending tests [3]. The measurement results for consoles on a substrate are also affected by the fixing conditions. The aim of the present study was to resolve the associated uncertainty of values of the Young's modulus of a console.

The diagram of a supported console beam (model I) is shown at the top of Fig. 1, *b*: the first span is fixed at point  $x = -L$  and supported at point  $x = 0$ ; the second span (console with length  $l$ ) is supported at point  $x = 0$ , and force  $F$  is applied at point  $x = X$ ,  $X \in (0, l]$ ; the Young's modulus is  $E$ , and the moment of inertia of the beam is  $I$ . The formula for console deflection  $z(x)$  in this statically indeterminate problem may be derived using the method of addition of the action of forces [8] (the derivation

of this formula is presented as a supplementary material in the online version of the paper). The formula is as follows:

$$z(x) = F \frac{3XLx + 6Xx^2 - 2x^3}{12EI}, \quad x \in [0, X], \quad X \in (0, l]. \quad (1)$$

Dependence (1) cannot be verified directly in an AFM. However, one may measure the stiffness or the deflection (deformation) of the console, which is inversely proportional to stiffness, at load point  $x = X$ :

$$z(X) = F \frac{3LX^2 + 4X^3}{12EI}. \quad (2)$$

Normalizing  $z(X)$  and  $X$  by the maximum  $z(l)$  and console length  $l$ , respectively, we find the formula for fitting

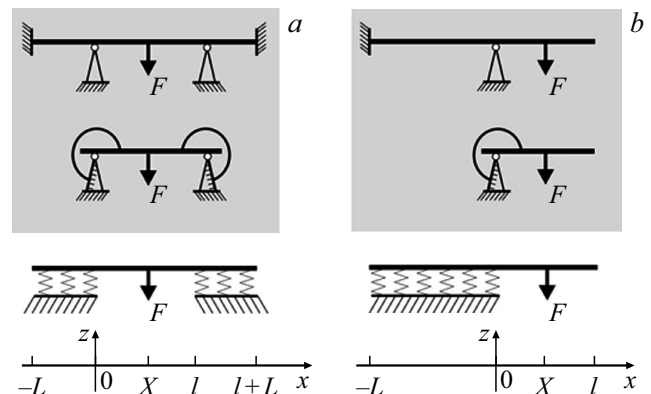


**Figure 1.** *a* — fixing conditions for a nanobridge: the diagrams of a three-span beam (top) and a beam on an elastic foundation (bottom) were considered in [5] and [7] (diagrams at the top and at the center (a beam on ring springs corresponding to boundary conditions  $z^{\text{II}}(0) = 4z^{\text{I}}(0)/L$  and  $z^{\text{II}}(l) = -4z^{\text{I}}(l)/L$  are equivalent). *b* — fixing conditions for a console (present study): model I — diagrams at the top and at the center, model II — diagram at the bottom.

Krylov's functions

$i$	$Y_i$	$K_i$
1	$Y_1(x) = \cosh x \cos x$	$K_1(x) = \frac{1}{2}(\cosh x + \cos x)$
2	$Y_2(x) = \frac{1}{2}(\cosh x \sin x + \sinh x \cos x)$	$K_2(x) = \frac{1}{2}(\sinh x + \sin x)$
3	$Y_3(x) = \frac{1}{2} \sinh x \sin x$	$K_3(x) = \frac{1}{2}(\cosh x - \cos x)$
4	$Y_4(x) = \frac{1}{4}(\cosh x \sin x - \sinh x \cos x)$	$K_4(x) = \frac{1}{2}(\sinh x - \sin x)$

the deflection profile to the experimental data for model I

$$\xi_I(\chi) = \frac{4}{4+3\lambda} \chi^3 + \frac{3\lambda}{4+3\lambda} \chi^2, \quad \chi = \frac{X}{l}, \quad \lambda = \frac{L}{l}, \quad (3a)$$

and, inserting  $X = l$  into Eq. (2), obtain the expressions for Young's modulus  $E$

$$E = \frac{F}{z(l)} \frac{l^3}{3I} \frac{4+3\lambda}{4} = E_0 \Phi_I, \quad (3b)$$

$$\Phi_I = \frac{4+3\lambda}{4}, \quad E_0 = \frac{F}{D^{\max}} \frac{64l^3}{3\pi d^4}.$$

Here,  $E_0$  is the Young's modulus of a rigidly fixed console,  $D^{\max} = z(l)$  is the maximum deformation,  $\Phi_I$  is the correction factor, and  $I = \pi d^4/64$  for a cylindrical beam with diameter  $d$ .

The diagram of model I is equivalent to a console on a ring spring (Fig. 1, *b*, center). Moment of force  $EIZ''$  [4] produced by the spring and console deflection angle  $z^I$  are linearly related. The deflection of such a console is governed by the solution of equation  $z^{IV} = 0$  with boundary conditions  $z(0) = 0$ ,  $z''(0) = 4z^I(0)/L$ ,  $z''(X) = 0$ ,  $z'''(X) = -F/EI$ . It is easy to verify (see also the supplementary materials in the online version of the paper) that the solution is formula (1).

The diagram of a beam on an elastic foundation with a suspended console (model II) is shown at the bottom of Fig. 1, *b*: the first span is on an elastic foundation  $x \in [-L, 0]$ , foundation modulus  $k_W$ ; the second span ( $x \in [0, l]$ ) is suspended. In the general case, the deflection of the first span [9] is characterized by a linear combination of  $z_1(x)$  Krylov's functions  $Y_i$  (see the table), and the beam deflection is characterized by polynomial  $z_2(x)$ :

$$z_1(x) = \sum_{i=1}^4 A_i Y_i(\beta x), \quad \beta = \sqrt[4]{\frac{k_W}{4EI}} = \sqrt[4]{\frac{16k_W}{\pi E}} d^{-1},$$

$$z_2(x) = \sum_{i=0}^3 a_i x^i. \quad (4)$$

The moment of inertia of a cylindrical beam section with diameter  $d$  was used for  $I$  in (4).

The analytical form of  $z_1(x)$  and  $z_2(x)$  was determined (see the supplementary materials in the online

version of the paper) and  $z_2(x)$  for boundary conditions  $z_1^I(-L) = z_1(-L) = 0$ ,  $z_1^{II}(0) = z_2^{II}(0)$ ,  $z_1^I(0) = z_2^I(0)$  and  $z_1(0) = z_2(0)$ ,  $z_2^{III}(X) = -F/EI$  and  $z_2^{II}(X) = 0$ .

The basic relations of model II: formula for fitting to experimental data

$$\xi_{II}(\chi) = [3K_4(2\beta_l \Lambda) + 6K_3(2\beta_l \Lambda)(\beta_l \chi) + 6K_2(2\beta_l \Lambda)(\beta_l \chi)^2 + 2(K_1(2\beta_l \Lambda) - 1)(\beta_l \chi)^3] [3K_4(2\beta_l \Lambda) + 6K_3(2\beta_l \Lambda)\beta_l + 6K_2(2\beta_l \Lambda)\beta_l^2 + 2(K_1(2\beta_l \Lambda) - 1)\beta_l^3]^{-1},$$

$$\Lambda = L/l, \quad \beta_l = \beta l; \quad (5a)$$

correction factor

$$\Phi_{II} = 1 + \frac{3K_4(2\beta_l \Lambda) + 6K_3(2\beta_l \Lambda)\beta_l + 6K_2(2\beta_l \Lambda)\beta_l^2}{2(K_1(2\beta_l \Lambda) - 1)\beta_l^3},$$

$$E = E_0 \Phi_{II}. \quad (5b)$$

Krylov's functions  $K_i$  are listed in the table.

Models I and II both have one fitting parameter:  $\lambda$  (see (3a)) and  $\beta_l$  (see (5a)); parameter  $\Lambda$  is known in each test. Factor  $\Phi_I$  may be infinite and is independent of the substrate stiffness. Factor  $\Phi_{II}$  is large at soft ( $\beta_l$  is small) substrates and  $\sim 1$  at rigid substrates. It is reasonable to expect that the Young's modulus values determined using model I will be higher than those provided by model II.

The procedure of AFM bend testing for a suspended object (models I and II) was applied to determine the Young's modulus of nanoscrolls of the  $\text{MgNi}_2\text{Si}_2\text{O}_5(\text{OH})_4$  composition. A suspension of nanoscrolls, which were obtained by hydrothermal synthesis [10], in isopropyl alcohol was prepared. A droplet of this suspension was deposited onto a TGZ2 silicon calibration grating (NT-MDT SI, Russia) and left to dry out. The samples were studied in the PeakForce QNM AFM mode of a BioScope Catalyst (Bruker, United States) instrument. In addition to deformation, the topography and peak force error signals, which are needed to correct the deformation values [6] for the contribution from the AFM probe slipping within sloped regions of the sample [11], were recorded. AFM data were processed in Gwyddion 2.55.

Two profiles were retrieved along a nanoscroll from the image of corrected deformation [5]. The suspended part of a nanoscroll in the topography image specified the length of the first profile; the length of the second profile was defined by the region of nonzero deformation. The profiles normalized vertically and horizontally were analyzed using models I and II for consoles and the algorithm [5] for bridges with fitting dependence

$$\xi(\chi) = 4^3(\chi - \chi^2)^3 \frac{2 + \lambda}{(1 + 2\lambda)(2 + 3\lambda)} + 4^2(\chi - \chi^2)^2 \frac{6\lambda(1 + \lambda)}{(1 + 2\lambda)(2 + 3\lambda)}, \quad (6a)$$

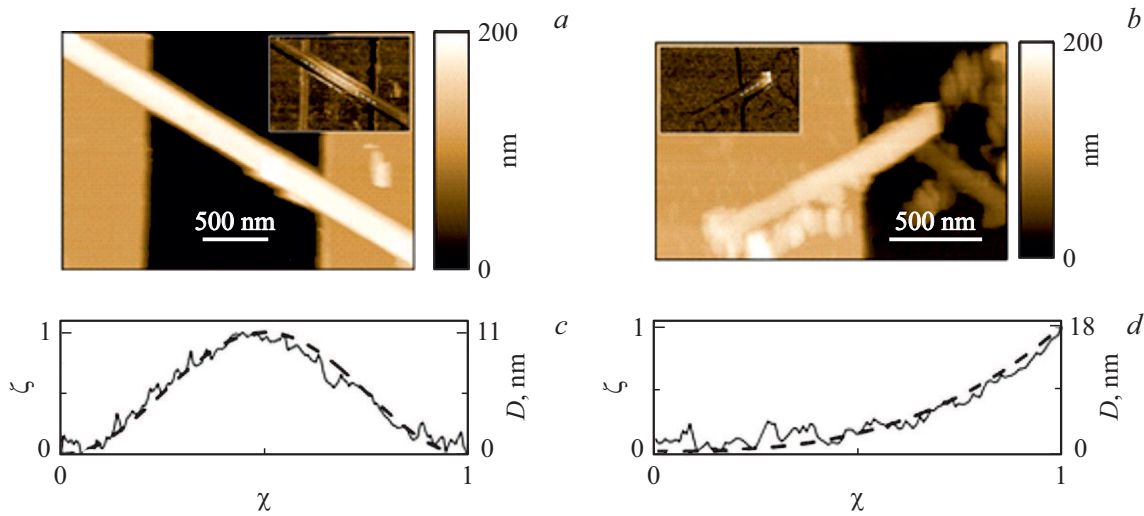


**Figure 2.** AFM data on the relief height within TGZ2 regions with  $\text{MgNi}_2\text{Si}_2\text{O}_5(\text{OH})_4$  nanoscrolls forming a bridge (a) and a console (b) (the corresponding data for the signal of corrected deformation  $D$  are shown in the insets; in both cases, the signal variation is 0–20 nm, and the profiles of  $D$  were retrieved along the dashed line) and normalized  $\xi(\chi)$  profiles of a bridge (c) and a console (d). The imaging parameters are as follows: the stiffness of FMG01 cantilevers is 2.4 (a, c) and 3.6 N/m (b, d); the frequency and the amplitude of vertical probe oscillations are 1 kHz and 150 nm; the horizontal scan rate is 0.3 Hz; and peak force  $F = 80$  (a, c) and 15 nN (b, d). In panel a, bridge span length  $l = 1701$  nm; in panel b, console length  $l = 417$  nm, and the length of the unsuspended beam part is  $L = 859$  nm.

and the following expressions for correction factor  $\Phi$  and Young's modulus  $E$ :

$$\Phi = \frac{4\lambda + 2}{\lambda + 2}, \quad E_{CB} = \frac{F}{D^{\max}} \frac{l^3}{3\pi d^4}, \quad E = E_{CB}\Phi, \quad (6b)$$

where  $E_{CB}$  is the Young's modulus for a fixed-end beam,  $\chi = X/l$ , and  $\lambda = L/l$  (see Fig. 1, a).

Out of the two deformation profiles, the profile better fitted (with a smaller residual) by curves (3a), (5a), or (6a) was chosen. The average height of the unsuspended part was taken as the external diameter ( $d$ ) of a nanoscroll. Inserting the fitting parameter, the suspended part dimensions, and the measured  $F/D^{\max}$  value into (3b), (5b), or (6b), we determined the needed  $E$  value.

Fig. 2 presents an example of AFM data for a bridge and a console. The Young's modulus of the bridge was  $E = 134$  GPa with fitting parameter  $\lambda = 0.42$  and correction factor  $\Phi = 1.52$  ( $l = 1701$  nm,  $d = 81$  nm,  $F/D^{\max} = 7.2$  N/m). The results of analysis of the console data with the use of model II were as follows:  $E = 63$  GPa,  $\beta_I = 5.47$ ,  $\Phi_{II} = 1.66$  ( $l = 417$  nm,  $d = 57$  nm,  $\Lambda = 2.06$ ,  $F/D^{\max} = 0.81$  N/m). The results for the same console provided by model I:  $E = 63$  GPa,  $\lambda = 0.87$ ,  $\Phi_I = 1.65$ . The exact match between the Young's modulus values was accidental.

Large values of  $\beta_I$  in model II and small values of  $\lambda$  in model I correspond to console deflection in accordance with the  $\chi^3$  law. Significant deviations from  $\chi^3$  were observed more often. According to model I, five out of 18 consoles deflected in accordance with the  $\chi^2$  law and had infinite  $\Phi_I$ . The value of  $E$  averaged over the remaining 13 consoles is  $E = 496 \pm 1057$  GPa ( $\Phi_I = 7.42 \pm 13.30$ ). The

Young's modulus for 12 studied bridges is  $\sim 4$  times lower:  $E = 134 \pm 148$  GPa ( $\Phi = 1.52 \pm 0.56$ ). The analysis of all 18 consoles with the use of model II did, in contrast, yield a value of  $E$  that agreed closely with the Young's modulus of bridges:  $E = 109 \pm 86$  GPa ( $\Phi_{II} = 3.05 \pm 1.15$ ). Therefore, the use of model II is preferable in tests of consoles.

Let us consider  $k_W$ , the coefficient relating the force per unit length to the displacement of an elastic foundation in model II. The value of  $(\beta_I d/l)^4$  averaged over 18 tests is 0.072. According to (4),  $(\beta_I d/l)^4 = 16k_W/\pi E$  and  $k_W = 0.014E$ . A rigid cylinder (nanoscroll with length  $L$ ), is indented to depth  $z_i$  into a soft substrate by force  $F_i$ :  $F_i/L \approx [\pi E_S/4(1-\nu_S^2)]z_i$  [12], where  $E_S$  and  $\nu_S$  are the Young's modulus and the Poisson's ratio of the substrate. Thus,  $E_S \approx k_W = 0.014E \approx 2$  GPa ( $E$  is the Young's modulus of a nanoscroll). Since the Young's modulus of projections of a  $\text{SiO}_2$  TGZ2 grating is 70 GPa, the value of  $E_S$  apparently characterizes the contamination of the grating and nanoscrolls.

We note in conclusion that a refined procedure for AFM bend testing of a suspended object was proposed. This procedure is sensitive to the conditions of fixing of the object on a substrate. Two models of fixing conditions of consoles were examined. Only the model of a beam on an elastic foundation with a suspended console provides results that agree with the Young's modulus of bridges.

## Acknowledgments

The authors would like to thank A.A. Krasilin for providing the samples of synthetic  $\text{MgNi}_2\text{Si}_2\text{O}_5(\text{OH})_4$  nanoscrolls and preparing them for AFM studies and M.B. Babenkov for his help in calculations.

## Funding

This study was supported financially by the Russian Science Foundation (grant No. 19-13-00151).

## Conflict of interest

The authors declare that they have no conflict of interest.

## References

- [1] J.-P. Salvetat, A.J. Kulik, J.-M. Bonard, G.A.D. Briggs, T. Stöckli, K. Méténier, S. Bonnamy, F. Béguin, N.A. Burnham, L. Forró, *Adv. Mater.*, **11** (2), 161 (1999). DOI: 10.1002/(SICI)1521-4095(199902)11:2<161::AID-ADMA161>3.0.CO;2-J
- [2] S. Cuenot, S. Demoustier-Champagne, B. Nysten, *Phys. Rev. Lett.*, **85** (8), 1690 (2000). DOI: 10.1103/PhysRevLett.85.1690
- [3] A. Kis, *Mechanical properties of mesoscopic objects*, PhD thesis (EPFL, Lausanne, 2003).
- [4] L.D. Landau, E.M. Lifshitz, *Theory of elasticity* (Pergamon, Oxford, 1970), p. 89.
- [5] A.V. Ankudinov, *Semiconductors*, **53** (14), 1891 (2019). DOI: 10.1134/S1063782619140021
- [6] M.M. Khalisov, V.A. Lebedev, A.S. Poluboyarinov, A.V. Garshev, E.K. Khrapova, A.A. Krasilin, A.V. Ankudinov, *Nanosyst: Phys., Chem., Math.*, **12** (1), 118 (2021). DOI: 10.17586/2220-8054-2021-12-1-118-127
- [7] D. Gangadean, D.N. McIlroy, B.E. Faulkner, D.E. Asto, *Nanotechnology*, **21**, 225704 (2010). DOI: 10.1088/0957-4484/21/22/225704
- [8] S.P. Timoshenko, *Soprotivlenie materialov: elementarnaya teoriya i zadachi* (Nauka, M., 1965), Vol. 1, p. 155 (in Russian).
- [9] A.N. Krylov, *O raschete balok, lezhashchikh na uprugom osnovanii* (Akad. Nauk SSSR, L., 1931), p. 24 (in Russian).
- [10] E.K. Khrapova, V.L. Ugolkov, E.A. Straumal, S.A. Lermontov, V.A. Lebedev, D.A. Kozlov, T.S. Kunkel, A. Nominé, S. Bruyere, J. Ghanbaja, T. Belmonte, A.A. Krasilin, *ChemNanoMat*, **7** (3), 257 (2021). DOI: 10.1002/cnma.202100018
- [11] A.V. Ankudinov, M.M. Khalisov, *Tech. Phys.*, **65** (11), 1866 (2020). DOI: 10.1134/S1063784220110031.
- [12] V.L. Popov, *Contact mechanics and friction: physical principles and applications* (Springer, Germany, 2017), p. 57. DOI: 10.1007/978-3-662-53081-8\_18